Ruthenium(II) phosphine/diimine/picolinate complexes: inorganic compounds as agents against tuberculosis

European Journal of Medicinal Chemistry, Issy le Moulineaux : Elsevier Masson, v. 46, n. 10, p. 5099-5107, Oct. 2011

European Journal of Medicinal Chemistry 46 (2011) 5099–5107

Contents lists available at SciVerse ScienceDirect

European Journal of Medicinal Chemistry

journal homepage: http://www.elsevier.com/locate/ejmech

Original article

Ruthenium(II) phosphine/diimine/picolinate complexes: Inorganic compounds as agents against tuberculosis

Fernando R. Pavan [a,*], Gustavo V. Poelhsitz [b], Marilia I.F. Barbosa [c], Sergio R.A. Leite [d], Alzir A. Batista [c,**], Javier Ellena [e], Leticia S. Sato [a], Scott G. Franzblau [f], Virtudes Moreno [g], Dinorah Gambino [h], Clarice Q.F. Leite [a,*]

[a] Faculdade de Ciências Farmacêuticas, Universidade Estadual Paulista, CEP 14801-902, Araraquara, SP, Brazil
[b] Instituto de Química, Universidade Federal de Uberlândia, CEP 38400-902, Uberlândia, MG, Brazil
[c] Departamento de Química, Universidade Federal de São Carlos, CEP 13565-905, São Carlos, SP, Brazil
[d] Instituto de Química, Universidade Estadual Paulista, CEP 14800-900, Araraquara, SP, Brazil
[e] Instituto de Fisica de São Carlos, Universidade de São Paulo, CEP 13560-970, São Carlos, SP, Brazil
[f] Institute for Tuberculosis Research, College of Pharmacy, University of Illinois at Chicago, Chicago, IL, USA
[g] Department de Química Inorgânica, Universitat de Barcelona, Marti y Franquès 1-11, 08028, Barcelona, Spain
[h] Cátedra de Química Inorgánica, Departamento Estrella Campos, Facultad de Química, Universidad de La República, Gral. Flores 2124, 11800 Montevideo, Uruguay

ARTICLE INFO

Article history:
Received 26 April 2011
Received in revised form
16 August 2011
Accepted 16 August 2011
Available online 23 August 2011

Keywords:
Mycobacterium tuberculosis
Drug resistance
Ruthenium
Phosphine/diimine/picolinate

ABSTRACT

This paper describes the synthesis and characterization of four new ruthenium complexes containing 1,4 bis(diphenylphosphino)butane (dppb), 2-pyridinecarboxylic acid anion (pic) and the diimines [(2,2′-bipyridine (bipy), 4,4′-dimethyl-2,2′-bipyridine (Me-bipy), 4,4′-dichloro-2,2′-bipyridine (Cl-bipy) and 1,10-phenanthroline (phen) as ligands, with formulae [Ru(pic)(dppb)(bipy)]PF_6 (**SCAR01**), [Ru(pic)(dppb)(Me-bipy)]PF_6 (**SCAR02**), [Ru(pic)(dppb)(Cl-bipy)]PF_6 (**SCAR03**) and [Ru(pic)(dppb)(phen)]PF_6 (**SCAR04**). Additionally, the *in vitro* anti-*Mycobacterium tuberculosis* (MTB) activity, cytotoxicity and activity against *in vitro* infection of these complexes and two more complexes, *cis*-[Ru(pic)(dppe)$_2$]PF_6 (**SCAR05**) and *cis*-[$RuCl_2$(dppb)(bipy)] (**SCAR06**), and their free ligands are described and discussed. All compounds showed excellent MIC against MTB, low cytotoxicity and a selectivity index higher than 10. Also, all compounds showed significant intracellular inhibition and the compound **SCAR05** showed a better activity than rifampin and SQ109. This is the first report of activity against *in vitro* infection of ruthenium compounds.

1. Introduction

The tuberculosis (TB) mortality rates decreased globally in 2007, with 1.3 million HIV-negative TB patients dying in 2007 and 456,000 deaths among individuals infected with both TB and HIV. However, in 2007 there were an estimated 9.27 million incident cases of TB, the majority of which occurred in Asia and Africa. This is an increase from the previous year, when 9.24 million cases were recorded [1]. In addition, the highly drug-resistant organisms are virtually untreatable in immunocompetent patients, so when these organisms enter into contact with highly immunocompromised HIV-infected populations, the mortality rate within a few weeks of infection approaches 100% [2]. In the last 40 years, no new drugs have been developed specifically against mycobacteria [3] and, only in the last few years, some promising candidate drugs are being tested in the preclinical phase [4]. Thus, there is a great need to develop new therapeutic agents to treat tuberculosis, so as to reduce the total duration of treatment and to provide more effective treatment against multidrug resistance (MDR), extensive drug resistance (XDR) and latent tuberculosis infection [5]. There are currently two main approaches to developing a new anti-TB drug [6]. One of them is based on the synthesis of analogues of existing drugs, with the aim of shortening and improving TB treatment. The other involves a search for novel structures with which mycobacteria have never been challenged before [7]. Adopting this second approach, our research is focused on the synthesis and characterization of new compounds, specifically new metal complexes.

Medicinal chemistry is taking a growing interest in the development of metal complexes for use as drugs or diagnostic agents.

* Corresponding authors. Tel.: +55 16 33016953.
** Corresponding author. Tel.: +55 16 33518285.
E-mail addresses: pavanfer@yahoo.com.br (F.R. Pavan), daab@power.ufscar.br (A.A. Batista), leitecqf@fcfar.unesp.br (C.Q.F. Leite).

0223-5234/$ – see front matter © 2011 Elsevier Masson SAS. All rights reserved.
doi:10.1016/j.ejmech.2011.08.023

Owing to their wide spectrum of coordination numbers and geometries, as well as kinetic properties, metal compounds offer mechanisms of drug action that cannot be realized by organic agents [7,8]. Ruthenium compounds have already exhibited potential anti-tumour activity since the 1970s and 1980s, and, more recently, the Ru(III) complexes NAMI-A and KP 1019 (FFC14a) have entered clinical trials. Recent studies have indicated that the anti-tumour activity of Ru(III) complexes also depends on their reducibility to Ru(II) species. The *in vitro* activity of a homologous series of Ru(III) complexes increased with increasing ease of reduction [8].

In this laboratory, we have studied and reported on the anti-*Mycobacterium tuberculosis* (MTB) activity of several new complexes containing various metals [3,7,9–14]. Specifically, Ru(II) complexes have shown excellent activity against *in vitro* MTB, being up to 150 times more active than their free ligands 4,6-dimethyl-2-mercaptopyrimidine; 1,4 bis(diphenylphosphino)butane; 1,2-bis(diphenylphosphio)ethane, bis(diphenylphosphino) methane, triphenylphosphine, 2,2′-bipyridine, 4,4′-dimethyl-2,2′-bipyridine, 2-pyridinecarboxylic acid and, interestingly, in these complexes the activity was higher, when they contained three chelated ligands, than that of the precursor complexes containing two chelated and two chloride ligands [9,14].

This paper describes the synthesis and characterization of four new ruthenium(II) complexes containing 1,4 bis(diphenylphosphino)butane (dppb), the 2-pyridinecarboxylic acid anion (pic) and diimines (bipy, Me-bipy, Cl-bipy and phen) as ligands, with formulae [Ru(pic)(dppb)(bipy)]PF_6 (**SCAR01**), [Ru(pic)(dppb)(Me-bipy)]PF_6 (**SCAR02**), [Ru(pic)(dppb)(Cl-bipy)]PF_6 (**SCAR03**) and [Ru(pic)(dppb)(phen)]PF_6 (**SCAR04**). Additionally, the *in vitro* anti-*M. tuberculosis* (MTB) activity, cytotoxicity and activity against *in vitro* infection of these complexes and two more complexes, *cis*-[Ru(pic)(dppe)$_2$]PF_6 (**SCAR05**) and *cis*-[$RuCl_2$(dppb)(bipy)] (**SCAR06**) [9,15], and their free ligands are presented and discussed.

2. Results and discussion

2.1. Synthesis of the complexes

The chemical reactivity of the 2-pyridinecarboxylic acid (Hpic) ligand with complexes such as *cis*-[$RuCl_2$(dppb)(N-N)] [15] enabled the synthesis of complexes with the general formula [Ru(pic)(dppb)(N–N)]PF_6 (N-N = bipy, Me-bipy, Cl-bipy or phen), containing three chelated ligands, under mild conditions, by simple chloride exchange (see Scheme 1).

2.2. Structural studies

The X-ray structure of **SCAR01** was determined and an ORTEP view showing the atom numbering scheme is shown in Fig. 1. Selected bond lengths and angles are presented in Table 1. The crystal structure of the complex consists of separate discrete molecular units and solvated water molecules (w). Complex

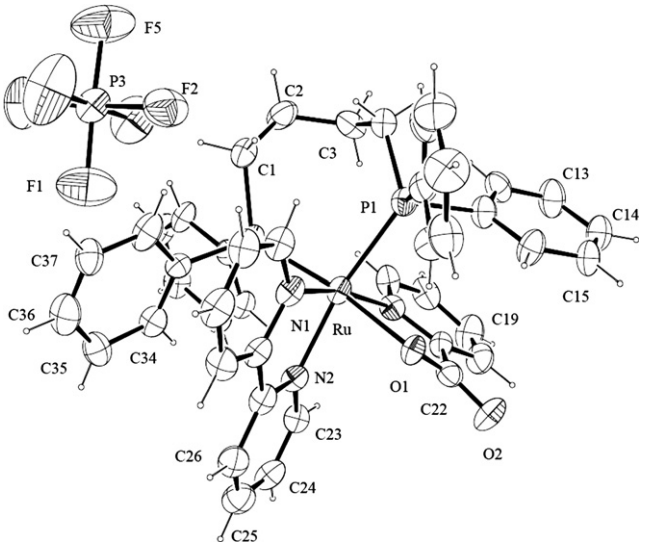

Fig. 1. *ORTEP* view of the cation complex [Ru(pic)(dppb)(bipy)]$PF_6 \cdot 2H_2O$ (**SCAR01**) showing the labels and 50% probability ellipsoids of the atoms. The solvent molecules were omitted.

SCAR01 crystallizes in the monoclinic system, space group $P2_1/n$, the Ru center being coordinated by three bidentate ligands in a distorted octahedral geometry as shown by the angles around the metal ion, listed in Table 1. One phosphorus atom is disposed *trans* to one nitrogen atom of the bipy and the other *trans* to the oxygen of the pic ligand.

The Ru–P bond lengths of 2.3256(18) and 2.350(2) Å are within the normal range found for Ru(II) tertiary phosphine complexes [15–19]. The P–Ru–P angle in the seven-member ring of dppb is 99.36(7)°, comparable with the values previously observed for the precursor **SCAR05** [15]. The average Ru-N (bipy) distance of 2.099 Å in complex **SCAR01** is also similar to that observed in **SCAR05** (2.09 Å) [15]. The Ru-N(3) and Ru–O(1) distances of the pic ligand, of 2.116(5) and 2.132(5)Å, respectively, are similar to those observed in other Ru(II) complexes containing this ligand [20,21]. The pic ligand dimensions in complex **SCAR01** (C(22)–O(1) = 1.274(9) Å, C(22)-O(2) = 1.219(9) Å) are consistent with deprotonation and coordination of the heterocycle to the Ru center [20,21]. The five-membered ring formed by the O-,N- chelating heterocyclic picolinate is inherently strained [20,21]. This is corroborated in **SCAR01** by the small O(1)–Ru–N(3) angle of 77.9(2)°.

2.3. Characterization of the compounds

The $^{31}P\{^1H\}$ NMR spectra of complexes **SCAR01-4** in CH_2Cl_2/D_2O in a capillary presented typical AB spin systems exhibiting chemical shifts close to 39.0 (d) and 37.3 (d), with $^2J_{P\text{-}P} = 33.5$ Hz, indicating the magnetic nonequivalence of the two phosphorus atoms

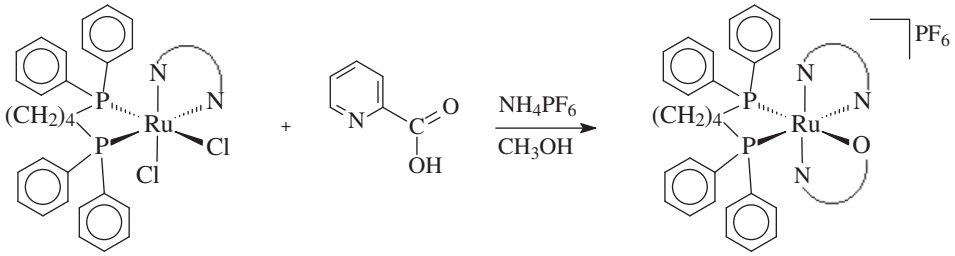

Scheme 1. Synthesis of the ruthenium(II) compounds containing the pic ligand.

Table 1
Selected bond lengths (Å) and angles (°) for complex [Ru(pic)(dppb)(bipy)]$PF_6 \cdot 2H_2O$ with standard deviations in parentheses.

Ru–N(1)	2.088(6)	N(1)–Ru–N(2)	79.6(3)	N(3)–Ru–0(1)	78.3(2)
Ru–N(2)	2.094(7)	N(1)–Ru–N(3)	167.9(3)	O(1)–Ru–P(2)	172.30(17)
Ru–N(3)	2.112(6)	N(2)–Ru–N(3)	93.0(2)	O(1)–Ru–P(1)	87.96(18)
Ru–O(1)	2.122(5)	N(1)–Ru–O(1)	91.0(2)	N(1)–Ru–P(1)	96.0(2)
Ru–P(1)	2.347(3)	N(2)–Ru–O(1)	79.9(2)	N(2)–Ru–P(1)	166.99(17)
Ru–P(2)	2.324(2)	N(3)–Ru–O(1)	78.3(2)	N(3)–Ru–P(1)	89.1(2)
O(1)–C(22)	1.282(10)	N(1)–Ru–P(2)	85.60(18)	N(3)–Ru–P(2)	104.37(18)
O(2)–C(22)	1.211(11)	N(2)–Ru–P(2)	92.64(19)	P(2)–Ru–P(1)	99.25(9)

(complete data in Table 2). Precursor complexes of general formula *cis*-[$RuCl_2$(dppb)(N-N)] show a pair of doublets at 43.0 and 32.0 ppm, with $^2J_{P\text{-}P} = 32.0$ Hz, in their $^{31}P\{^1H\}$ spectra [15,22]. In the precursors, the high-field doublet corresponds to the P *trans* N, as previously described [15]. These assignments are based on an empirical linear correlation established between the crystallographically determined Ru–P distances in a series of Ru-dppb complexes and the corresponding ^{31}P chemical shifts observed in solution, in which the chemical shifts become more high-field with increasing Ru–P bond length [15,16,19]. In light of this information, we suggest that in the new complexes the high-field doublet belongs to the P *trans* to nitrogen from bipy (N-N), because the Ru-P1 distance of 2.347(3) Å (*trans* N-N) is longer than that observed for the Ru-P2 *trans* O of the pic ligand (2.324(2) Å) (see Table 1).

The mass spectra (ESI-MS) of complexes **SCAR01-4**, delivered in a CH_2Cl_2 solution, showed the parent molecular ions at *m*/*z* values $[M - PF_6]^+$ consistent with the assigned formulation (see experimental data). No fragmentation was observed under the experimental conditions described.

The IR spectra of the new complexes also confirmed the presence of the pic ligand coordinated to the Ru(II) center. Bands corresponding to the ν_{as}(COO) and ν_s(COO) vibrational modes appeared close to 1660 and 1334 cm^{-1}, respectively, for all complexes. The band attributable to ν(OH), which appeared at 3200-3100 cm^{-1} in the free ligand spectrum, was absent in those of complexes **SCAR01-4**, indicating that the pic ligand is coordinated in the deprotonated form [23]. The electronic spectra of **SCAR01-4** complexes showed four absorptions in the UV region (two bands and two shoulders), assigned as intra-ligand transitions by means of comparison with the free ligands (dppb, N–N and pic). In the visible region, one band and a shoulder were observed, respectively close to 420 and 490 nm. These absorptions can be attributed to metal-to-ligand charge transfer transitions, probably involving both diimine (N–N) and pic ligands. The electrochemical behavior of these new complexes in cyclic voltammetric experiments was similar to that observed for their precursors [15,29]. A quasi-reversible one-electron Ru^{II}/Ru^{III} redox process was observed for each complex. As expected, the $E_{1/2}$ values found for the new complexes were considerably more anodic than those observed for the respective precursors, by approximately 0.60 V (Table 2), indicating that the Ru center was more stable in the new derivatives than in their precursors. This stabilization is assumed to be due to the replacement of two monoanionic donor chlorides by a single monocharged chelating pic unit, resulting in positively-charged product complexes [24]. Among the four new complexes, the $E_{1/2}$ values clearly correlate with the diimine pKa values, such that the complex containing the most acidic ligand (Cl-bipy) showed the most stable ruthenium center (highest $E_{1/2}$).

Table 2
$^{31}P\{^1H\}$ NMR and electrochemical data for complexes **SCAR01-4**.

Complex	δ (ppm)	$E_{1/2}$/V[a]	ΔE_p/V[b]	pKa (N-N)
SCAR01	P_A (37.8)/P_B (39.5)	1.21	0.21	4.44
SCAR02	P_A (37.2)/P_B (39.1)	1.14	0.17	4.92
SCAR03	P_A (36.8)/P_B (38.5)	1.32	0.19	2.61
SCAR04	P_A (38.0)/P_B (40.2)	1.22	0.13	4.27

[a] Scan rate: 100 mV s^{-1}.
[b] $\Delta E_p = E_{pa} - E_{pc}$.

2.4. Anti-M. tuberculosis activity assay

The *in vitro* anti-MTB activities of the free ligands and the phosphine-diimine-picolinate ruthenium complexes were tested against MTB $H_{37}Rv$ ATCC 27294 and the MICs are reported in Table 3. The MICs of complexes **SCAR01-05** are comparable to or better than those of some "second" and "first" line drugs used in current therapy [6,25,26]. SQ 109, an antitubercular compound derived from ethambutol, with MIC of 1.56 μM [27], and TMC 207, a diarylquinoline with MIC of 0.81 μM [28], both of which are new promising drug candidates, presently in the human clinical trial phase, are examples of *in vitro* activity comparable to the ruthenium complexes presented here. Even though the complex **SCAR06** showed the worst inhibitory result among the tested compounds, it had activity comparable to or better than the "second" line drugs [25]. Comparing the complexes **SCAR01** and **SCAR06**, we observe that **SCAR01** is 5.5 times more active than **SCAR06**, probably due to the absence of the Hpic ligand in the latter. The ligands dppe and phen are the only ones that have good MICs (15.70 and 11.80 μM respectively). However, these values are respectively 71 and 16 times higher than those of their complexes.

2.5. In vitro cytotoxicity

The cytotoxicity results (Table 3), expressed as the IC_{50} for the J774A.1 cell line, show that all of the tested ruthenium complexes exhibited low cytotoxicity (IC_{50} ranging from 3.4 to 104 μM). The free ligands are also not very cytotoxic (IC_{50} ranging from ≤50 to 2538 μM). The selectivity index (SI) of each compound was determined as the ratio of IC_{50} to MIC (Table 3). According to Orme et al. [29], candidates for new drugs must have an index equal to or higher than 10, together with MIC lower than 6.25 μg/mL (or the molar equivalent) and a low cytotoxicity. SI is used to estimate the therapeutic window of a drug and to identify drug candidates for further studies. Thus, all the ruthenium complexes studied here, with SI ranging from 15.20 to 40.10, are very promising new anti-tuberculosis drug candidates, and therefore they were all tested in the *in vitro* infection model [29].

2.6. In vitro infection model

The *in vitro* intracellular activities of the phosphine-diimine-picolinate ruthenium complexes were tested against MTB Erdmann (ATCC 35801) containing the Luciferase Plasmid and the inhibitory values are reported in Table 4. The compounds were tested in macrophages at those concentrations: at their MICs and 4 times higher and lower. All complexes presented significant intracellular activity at various concentrations. The complexes **SCAR02** and **SCAR05** were the most active because they showed the best activity at lower concentrations (0.13 μM = 70.50% inhibition and 0.06 μM = 47.60% inhibition, respectively). These complexes also exhibited the best activity at concentrations equal to and higher than the MIC. The comparison between the intracellular activity of compound **SCAR05** and rifampin (Table 4) showed a higher activity in the new compound. Additionally, the intracellular activities of compounds **SCAR01-05** are better than those of 26 synthesized compounds from a combinatorial library of 1,2-ethylenediamines, and comparable to SQ 109 (4.72 μM = 99% intracellular inhibition),

Table 3
Anti-MTB activity (MIC), cytotoxicity (IC_{50}), and selectivity index (SI) of the ruthenium complexes and their free ligands.

Identification	Compounds	MIC		IC_{50}		SI
		μg/mL	μM	μg/mL	μM	IC_{50}/MIC
SCAR01	[Ru(pic)(dppb)(bipy)]PF_6	0.91	0.95	31.30	32.60	34.20
SCAR02	[Ru(pic)(dppb)(Me-bipy)]PF_6	0.49	0.50	11.70	11.90	23.90
SCAR03	[Ru(pic)(dppb)(Cl-bipy)]PF_6	0.78	0.76	31.30	30.40	40.10
SCAR04	[Ru(pic)(dppb)(phen)]PF_6	0.63	0.74	19.50	23	31.20
SCAR05	*cis*-[Ru(pic)(dppe)$_2$]PF_6	0.26[a]	0.22[a]	3.90	3.35	15.20
SCAR06	*cis*-[$RuCl_2$(dppb)(bipy)]	3.90[a]	5.17[a]	78.20	104	20.10
Ligand	Hpic	> 50[a]	>406[a]	312.50	2538	≤ 6.25
Ligand	dppb	> 50[a]	>117.20[a]	625	1465	≤ 12.50
Ligand	dppe	6.25[a]	15.70[a]	156.30	392.6	25
Ligand	phen	2.34	11.80	≤ 9.80	≤ 50	≤ 4.20
Ligand	bipy	25[a]	160.10[a]	≤ 9.80	≤ 63	≤ 0.40
Ligand	Me-bipy	25[a]	135.70[a]	≤ 9.80	≤ 53.20	≤ 0.40
Ligand	Cl-bipy	25	111.06	19.50	86.63	0.78

[a] Data reported previously [9,14].

which is the best compound in this library [27]. On the other hand, the compound **SCAR06** showed low intracellular activity at 1.29 μM (19.40%), compared to the similar compound **SCAR01**, with 55.10% inhibition at a concentration of 0.95 μM (Table 4). This finding corroborates the previous observation about the importance of the presence of Hpic in the complex structure, to intensify the anti-tuberculosis activity.

2.7. *In vitro structure–activity–relationship (SAR)*

Indeed, although Hpic is the ligand with the lowest activity among the tested ligands against MTB, its presence in the ruthenium complexes increased both extra and intracellular activities. For example, the substitution of the two Cl atoms by Hpic in the *cis*-[$RuCl_2$(dppb)(bipy)] (**SCAR06**), resulting in [Ru(pic)(dppb)(bipy)]PF_6 (**SCAR01**), increased the anti-TB activity five times. Therefore, it is likely that the structures of the complexes are responsible for the properties of the compounds, and important for their mechanism of action as tuberculostatics. The structural changes probably affect the reaction of the complexes with bacterial DNA, which is the likely target of these drugs. It is known that the interaction with DNA is the basis of the cytostatic effect of ruthenium compounds [30–32] and this interaction is modulated by the nature of the ligands present in the complexes. In the present case, the smaller partial electronic charge on the free oxygen atom of the pic ligand, in comparison with the charges on the chlorine atoms of the original compound [33], makes the former the worst hydrogen bond acceptor. This could be associated with a higher cytotoxicity [32] and probably the anti-MTB effect follows the same trend.

In order to preliminary address if interaction with DNA could be part of the mode of action of the complexes, experiments with CT DNA were carried out. Binding of **SCAR01** to DNA was studied by combining atomic absorption determinations (for the metal) and electronic absorption measurements for DNA quantification. The complex showed a negligible covalent binding level to CT DNA (nmol Ru/mg DNA base pairs ≅ 0). Interaction with DNA was further explored through circular dichroism technique, viscosity measurements and atomic force microscopy (AFM). In Fig. 2, the circular dichroism spectra of **SCAR01** at several ruthenium complex: DNA molar ratios are shown. After 24 h of incubation at 37 °C, changes in molar ellipticity can be observed for the complex.

Table 4
Intracellular activity against MTB Erdmann ATCC 35801 with pSMT1 plasmid, of ruthenium compounds and rifampin at various concentrations.

Identification	Compounds	Concentrations Range		Intracellular inhibitory activities (%)
		μg/mL	μM	
SCAR01	[Ru(pic)(dppb)(bipy)]PF_6	3.64	3.80	77.50
		0.91	0.95	55.10
		0.23	0.24	48.30
SCAR02	[Ru(pic)(dppb)(Me-bipy)]PF_6	1.96	2	82.30
		0.49	0.50	73.30
		0.12	0.13	70.50
SCAR03	[Ru(pic)(dppb)(Cl-bipy)]PF_6	3.12	3.04	62.30
		0.78	0.76	43.30
		0.20	0.19	31.90
SCAR04	[Ru(pic)(dppb)(phen)]PF_6	2.52	2.96	78.90
		0.63	0.74	75.30
		0.16	0.19	65.90
SCAR05	*cis*-[Ru(pic)(dppe)$_2$]PF_6	1.04	0.88	85.20
		0.26	0.22	80.50
		0.07	0.06	47.60
SCAR06	*cis*-[$RuCl_2$(dppb)(bipy)]	15.6	20.70	51.10
		3.90	5.17	33.40
		0.98	1.29	19.40
RMP	Rifampin	0.40	0.49	80.40
		0.10	0.12	51.50
		0.03	0.04	24

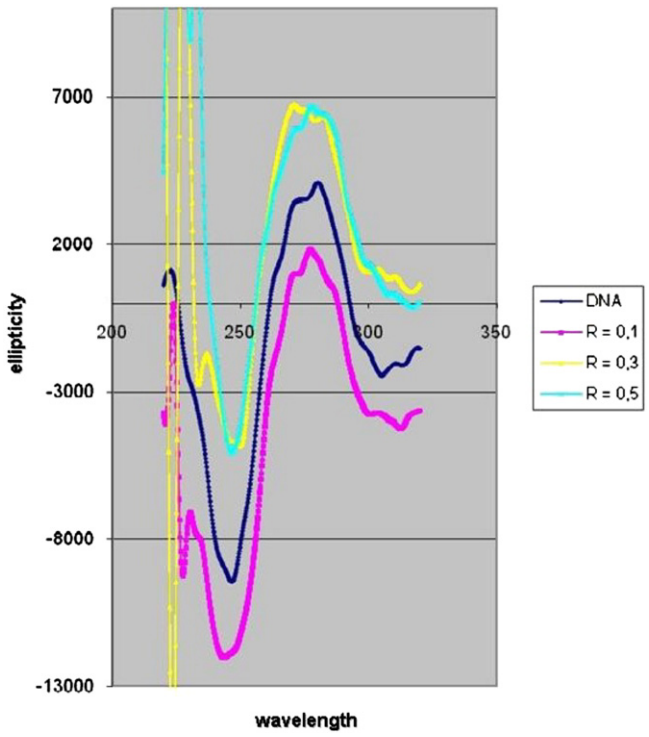

Fig. 2. Circular Dichroism spectra of plasmid ρBR322 DNA and plasmid ρBR322 DNA incubated with the [Ru(pic)(dppb)(bipy)]PF_6 (**SCAR01**) complex for 24 h, at 37 °C at molar ratios 0.1, 0.3 and 0.5.

These changes in the wavelength and the ellipticity of free DNA indicate modifications in the secondary structure of DNA as a consequence of its interaction with the complexes. Although the substitution of ligands by N atoms of DNA bases could be responsible, the most probable hypothesis is that weak interactions occur between the ligands and DNA, through hydrogen bonds.

The comparison of the AFM images of pBR322 DNA incubated with **SCAR01** (Fig. 3a) and of the free plasmid (Fig. 3b), show typical modifications in the form of the DNA, namely super coiling, kinks and compaction. These modifications indicate that **SCAR01** interacts with DNA. Additionally, the variation of viscosity with time at 25 °C shows a decrease in the viscosity, which implies that there is no intercalation of the complex between base pairs of the DNA. All these results are in agreement with the structure of **SCAR01** that seems not to allow neither covalent binding to DNA bases nor intercalation between bases.

It is known from the literature, that the KP1019 compound, a tumour-inhibiting drug with a new mode of action, which probably involves accumulation in transferrin receptor-(over) expressing tumour cells via transferrin receptor, subsequent reduction to Ru^{II} species, reacts with DNA and induction of apoptosis via intrinsic mitochondrial pathway [34]. Bratsos et al., presented some ruthenium complexes containing 1-(2-Picolyl)-substituted 1,2,3-triazole ligands showing their anticancer properties probably involving hydrolysis of the chloride ligand and subsequent reaction with DNA [35]. Furthermore, another recent study showed the cellular uptake and subcellular distribution including adduct formation with genomic DNA and uptake into mitochondria of two ruthenium(III)-based drugs in clinical trials, KP1019 and NAMI-A, indicating that these ruthenium drugs have distinct differences with respect to cisplatin, especially cisplatin-resistant cells. In comparison to the sensitive cells, KP1019 exhibits higher cytotoxicity and a slightly changed metabolism of the drug, whereas NAMI-A treatment results in increased intracellular ruthenium levels and a higher number of ruthenium-DNA adducts [36]. These data show that in fact the DNA can be a target for ruthenium complexes but interaction with proteins cannot be discarded as possible targets for ruthenium and other metal ions complexes.

The structures of the complexes studied in this work are quite different to the compounds containing chloride in their coordination sphere, what cause different interactions with the DNA. In this case only the complex **SCAR06** presents chloride coordinated to the ruthenium, but it was showed that only one *trans* to the phosphorus atom is dissociated from the metal [37,38].

In a previous study we reported that for the complexes [$Ru^{III}Cl_4$(DMSO)(H-Hypoxanthine)] and [$Ru^{III}Cl_4$(DMSO)[H-(N6-butyladenine)] was possible to observe in the AFM images a strong aggregation in plasmidic DNA forms [39]. No nuclease activity was observed in any of these tested complexes and the modifications observed confirm that these complexes do not destroy the structure of the pBR322 plasmid DNA but they yield more coiled and/or more associated plasmids. As in that case, in our present work we can observe aggregation of the forms but in a lower degree; the complex does not destroy the structure of the pBR322 plasmid DNA, no nuclease activity is observed. The compacting of the forms, the supercoiled observed, are in good agreement with the modification observed in CD spectrum and viscosity

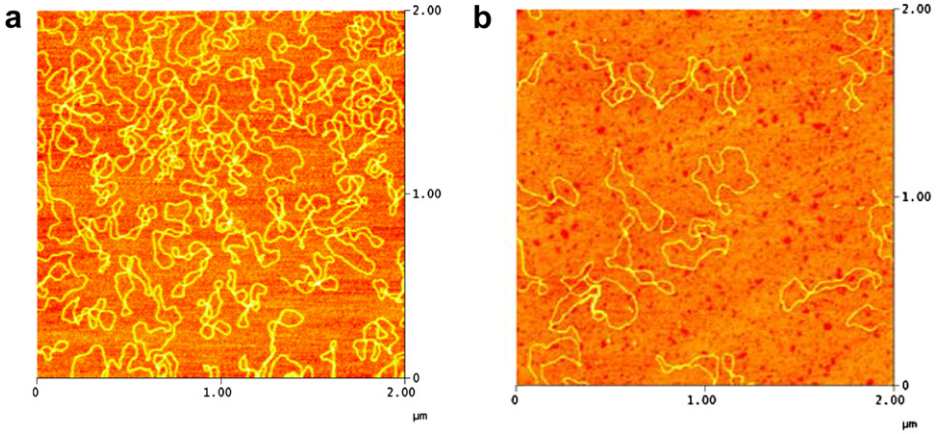

Fig. 3. (a) AFM image of the plasmid ρBR322 DNA incubated with the [Ru(pic)(dppb)(bipy)]PF_6 (**SCAR01**) complex for 24 h, at 37 °C. (b) AFM image of the free ρBR322 DNA.

measurements, which indicate interaction of the compound with DNA, probably by electrostatic forces.

3. Conclusions

The synthesis and characterization of four new ruthenium complexes has been described in this work. Additionally, biological studies of these four ruthenium complexes and two other ones together with those of the free ligands were presented. The results reported here confirm the biological activity of these ruthenium complexes and raise the possibility of these compounds becoming new drugs against TB.

4. Experimental section

4.1. Materials for synthesis

Solvents were purified by standard methods. All chemicals used were of reagent grade or comparable purity. $RuCl_3 \cdot 3H_2O$, the ligands 1,4-bis(diphenylphosphino)butane (dppb), 2,2′-bipyridine (bipy), 4,4′-dimethyl-2,2′-bipyridine (Me-bipy), 4,4′-dichloro-2,2′-bipyridine (Cl-bipy), 1-10-phenanthroline (phen) and 2-pyridinecarboxylic acid (Hpic) were used as received from Aldrich. The complexes *cis*-[$RuCl_2$(dppb)(N-N)], N-N = bipy, Me-bipy, Cl-bipy or phen were prepared according to published procedures [15,22].

4.2. Instrumentation

The infrared spectra were collected from CsI pellets in a Bomem-Michelson 102 FTIR spectrometer, in the 4000–200 cm^{-1} region. UV–visible (UV–Vis) spectra were recorded in a HP8452A (diode array) spectrophotometer. All NMR experiments were performed at 293 K in a Bruker spectrometer, 9.4 T, observing ^1H at 400.13, ^{13}C at 100.61 and $^{31}P\{^1H\}$ at 161.98 MHz. The NMR spectra were recorded in $CDCl_3$, with TMS (^1H and ^{13}C) and 85% H_3PO_4 ($^{31}P\{^1H\}$) as internal and external references, respectively. The splitting of proton, carbon and phosphorus resonances, respectively, in the reported ^1H, ^{13}C and $^{31}P\{^1H\}$ NMR spectra, are defined as d = doublet. Mass spectra were obtained in a QuattroLC Mass Spectrometer (Micromass, triple-quadrupole, ESI/APCI, UK) equipped with syringe pump (Phenix 40 pump, CE Instruments, Italy). The mobile phase used to deliver the sample into the ion source by direct infusion was dichloromethane (HPLC grade, JT Baker, Mexico) with 0.1% formic acid (v/v) (JT Baker, Mexico), flowing at 100 μL/min. All analyses were performed with an Electrospray Ionization (ESI) probe in the positive ion mode. In each analysis, 10 μL of a standard solution were injected at a concentration of 1 μg/mL. Cyclic voltammetry experiments were carried out at room temperature in CH_2Cl_2 containing 0.10 M Bu_4NClO_4 (TBAP) (Fluka Purum), with a Bioanalytical Systems Inc. BAS-100B/W electrochemical analyzer. The working and auxiliary electrodes were stationary Pt foils; a Luggin capillary probe was used and the reference electrode was Ag/AgCl. Under these conditions, ferrocene is oxidized at 0.43 V (Fc^+/Fc). C, H and N contents were determined in the Microanalytical Laboratory of Universidade Federal de São Carlos, São Carlos (SP), with an EA 1108 Fisions Instruments CHNS microanalyser.

Complexes were tested for their DNA interaction ability using native calf thymus DNA (CT DNA) (Type I) by a modification of a previously reported procedure [40,41]. CT DNA (50 mg) was dissolved in water (30 mL) (overnight). Solutions of the complexes in DMSO (spectroscopy grade) (1 mL, 10^{-3} M) were incubated at 37 °C with solution of CT DNA (1 mL) during 96 h. DNA/complexes mixtures were exhaustively washed to eliminate the un-reacted complex. Quantification of bound metal was done by atomic absorption spectroscopy on a Perkin Elmer 5000 spectrometer. Standards were prepared by diluting a metal standard solution for atomic absorption spectroscopy. Final DNA concentration per nucleotide was determined by UV absorption spectroscopy using molar absorption coefficient of 6000 M^{-1} cm^{-1} at 260 nm. The reported values are mean of three determinations. For the circular dichroism measurements, the **SCAR01** complex was dissolved in an aqueous solution (prepared with Milli-Q water) of 4% DMSO (2 mg compound/5 mL). The stock solutions were freshly prepared before use. The samples were prepared by the addition of aliquots of these stock solutions to the appropriate volume of CT DNA in a TE buffer solution (50 mM NaCl, 10 mM tris-(hydroxymethyl)aminomethane hydrochloride (Tris–HCl), 0.1 mM H_4edta, pH 7.4) (5 mL). The amount of complex added to the DNA solution was expressed as the input molar ratio of Ru to nucleotide, calculated by formula (1)

$$r_i = m.M_{nucl}.Am/C.Mr.V \quad (1)$$

where m = mass of the compound (g); M_{nucl} = mean nuclear mass per nucleotide (330 g/mol); Am = number of the metal atoms; C = concentration of DNA (g/mL); Mr = molar mass of the compound (g/mol); V = total volume of the sample (5 mL). A solution of free native DNA in TE was used as a blank. The CD spectra of DNA, in the presence and absence of complex (DNA concentration 20 mg/mL, molar ratios r_i = 0.10, 0.30, 0.50), were recorded at room temperature, after 24 h incubation at 37 °C, on a JASCO J-720 spectropolarimeter with a 450 W xenon lamp; a computer was used for spectral subtraction and noise reduction. Spectra for each sample were scanned twice, from 220 to 330 nm. The plotted CD spectra are the average of three independent scans. The data are expressed as average residue molecular ellipticity (θ) in degrees cm^2 $dmol^{-1}$. Viscosity experiments were carried out in an AND-SV-1 viscometer in a water bath with a water jacket, to maintain the temperature at 25 °C. A range of 200–370 μL of 5 mM solutions of the compound were added to 2 mL of 100 mM CT DNA

Table 5
Crystallographic data and refinement details for [Ru(pic)(dppb)(bipy)]$PF_6 \cdot 2H_2O$ (**SCAR01**).

Empirical formula	$C_{44}H_{40}N_3O_2P_2RuPF_6 \cdot 2H_2O$
Formula weight	986.80
Temperature (K)	293(2)
Crystal system	Triclinic
Space group	P-1
Unit cell dimensions	
a (Å)	9.8971(6)
b (Å)	10.4187(5)
c (Å)	21.9290(10)
α (°)	99.985(3)
β (°)	100.073(4)
γ (°)	95.853(3)
Volume (Å^3)	2172.12(19)
Z	2
Density (calculated) (g cm^{-3})	1.509
Absorption coefficient (mm^{-1})	0.543
F(000)	1008
Crystal size (mm^3)	0.27 × 0.25 × 0.20
θ range for data collection (°)	3.00–25.51
Limiting indices	$-11 \le h \le 11$ $-12 \le k \le 12$ $-26 \le l \le 26$
Reflections collected	11900
Independent reflections (R_{int})	7468 (0.0830)
Data/restraints/parameters	7468/0/560
Goodness-of-fit on F^2	1.004
Final R indices [$I > 2\sigma(I)$]	$R_1 = 0.0729$, $wR_2 = 0.1739$
R indices (all data)	$R_1 = 0.1208$, $wR_2 = 0.2359$
Peak and hole/e Å^{-3}	1.298 and −1.807

solution. The flow time was measured by a digital stop watch. For the Atomic Force Microscopy (TMAFM) experiment, plasmid pBR322 DNA was heated at 60 °C for 10 min to obtain the Open Circular form (OC form). Stock solution was 1 mg/mL in a buffer solution of HEPES (4 mM Hepes, pH 7.4/2 mM $MgCl_2$). Each sample contained 1 μL of pBR322 DNA at a concentration of 0.25 μg/μL, for a final volume of 40 μL. The amount of compound added is also expressed as r_i. AFM samples were prepared by placing a 3 μL drop of test solution onto freshly cleaved Muscovite green mica disks as the support. The drop was allowed to stand undisturbed for 3 min to favour the adsorbate–substrate interaction. Each DNA-laden disk was rinsed with Milli-Q water and blown dry with clean compressed argon gas directed normal to the disk surface. Samples were stored over silica gel prior to AFM imaging. All AFM observations were made with a Nanoscope III Multimode AFM (Digital Instruments, Santa Barbara, CA). Nano-crystal Si cantilevers of length 125 nm, with an average spring constant of 50 N/m, terminated with conical-shaped Si probe tips of apical radius 10 nm and cone angle 35° were utilized. High-resolution topographic AFM images were recorded in intermittent contact mode, at 1–3 Hz, in air at room temperature (relative humidity <40%), on various specimen areas of 2 × 2 μm.

4.3. X-ray crystallography

Orange [Ru(pic)(dppb)(bipy)]$PF_6 \cdot 2H_2O$ (**SCAR 01**) crystals were grown by slow evaporation of a dichloromethane/n-hexane solution. The crystal was mounted on an Enraf-Nonius Kappa-CCD diffractometer with graphite-monochromated Mo-Kα (λ = 0.71073 Å) radiation. The final unit–cell parameters were based on all reflections. Data collections were made with the COLLECT program [42]; integration and scaling of the reflections were performed with the HKL DENZO-SCALEPACK system of programs [43]. A semi-empirical (from equivalents) absorption correction was applied [43]. The structure was solved by direct methods with SHELXS-97 [44]. The model was refined by full-matrix least squares on F^2 by means of SHELXL-97 [45]. All hydrogen atoms were stereochemically positioned and refined with a riding model. The ORTEP view of **SCAR 01** is shown in Fig. 1 and was prepared with ORTEP-3 for Windows [46]. Hydrogen atoms on the aromatic rings were refined isotropically, each with a thermal parameter 20% greater than the equivalent isotropic displacement parameter of the atom to which it is bonded. The data collections and experimental details are summarized in Table 5. The determined bond lengths and angles are not sufficiently accurate for meaningful discussion; however, useful information may still be gleaned from the diffraction study with respect the coordination sphere of the metal.

4.4. Synthesis

The [Ru(pic)(dppb)(N-N)]PF_6 complexes (N-N = bipy, Me-bipy, Cl-bipy or phen) were prepared by allowing 50 mg (ca. 0.07 mmol) of the corresponding precursor *cis*-[$RuCl_2$(dppb)(N-N)] dissolved in 25 mL of methanol to react with excess 2-pyridinecarboxylic acid ligand (0.20 mmol; ≅24.6 mg) and 0.10 mmol (16.2 mg) of NH_4PF_6 under Ar atmosphere for 24 h. The final red solutions were concentrated to ca. 3 mL and water was added to precipitate an orange solid, which was filtered off, washed well with water (3 × 5 mL) and diethyl ether (3 × 5 mL) and dried *in vacuo*.

4.5. [Ru(pic)(dppb)(bipy)]PF_6 (**SCAR01**) yield

47 mg (75%). Anal. Calcd for $C_{44}H_{40}F_6N_3O_2P_3Ru$: exptl (calc) C, 55.12 (55.58); H, 4.74 (4.24); N, 4.46 (4.42). $^{31}P\{^1H\}$ NMR: δ(ppm) 39.5 (d); 37.8 (d), $^2J_{P\text{-}P}$ = 33.5 Hz. UV–Vis (CH_2Cl_2, 10^{-5} M): λ/nm (ε/M^{-1} cm^{-1}) 259sh (2.20 × 10^4), 290 (2.58 × 10^4), 301sh (2.22 × 10^4), 350sh (6.40 × 10^3), 422 (3.90 × 10^3), 490sh (1.60 × 10^3). ESI (m/z^+): 806 $[C_{44}H_{40}N_3O_2P_2Ru]^+$.

4.6. [Ru(pic)(dppb)(Me-bipy)]PF_6 (**SCAR02**) yield

54 mg (70%). Anal. Calcd for $C_{46}H_{44}F_6N_3O_2P_3Ru$: exptl (calc) C, 56.25 (56.44); H, 4.50 (4.53); N, 4.23 (4.29). $^{31}P\{^1H\}$ NMR: δ(ppm) 39.1 (d); 37.2 (d), $^2J_{P\text{-}P}$ = 33.5 Hz. UV–Vis (CH_2Cl_2, 10^{-5} M): λ/nm (ε/M^{-1} cm^{-1}) 260sh (1.87 × 10^4), 288 (2.20 × 10^4), 300sh (1.88 × 10^4), 352sh (5.90 × 10^3), 416 (3.90 × 10^3), 480sh (1.30 × 10^3). ESI (m/z^+): 834 $[C_{46}H_{44}N_3O_2P_2Ru]^+$.

4.7. [Ru(pic)(dppb)(Cl-bipy)]PF_6 (**SCAR03**) yield

61 mg (80%). Anal. Calcd for $C_{44}H_{38}F_6N_3O_2P_3RuCl_2$: exptl (calc) C, 51.73 (51.83); H, 4.17 (3.76); N, 4.21 (4.12). $^{31}P\{^1H\}$ NMR: δ(ppm) 38.5 (d); 36.8 (d), $^2J_{P\text{-}P}$ = 33.5 Hz. UV–Vis (CH_2Cl_2, 10^{-5} M): λ/nm (ε/M^{-1} cm^{-1}) 259sh (2.33 × 10^4), 294 (2.36 × 10^4), 337sh (9.60 × 10^3), 453 (4.50 × 10^3), 515sh (1.70 × 10^3). ESI (m/z^+): 874 $[C_{44}H_{38}N_3O_2P_2RuCl_2]^+$.

4.8. [Ru(pic)(dppb)(phen)]PF_6 (**SCAR04**) yield

56 mg (74%). Anal. Calcd for $C_{46}H_{40}F_6N_3O_2P_3Ru$: exptl (calc) C, 57.00 (56.68); H, 4.57 (4.14); N, 4.56 (4.31). $^{31}P\{^1H\}$ NMR: δ(ppm) 40.2 (d); 38.0 (d), $^2J_{P\text{-}P}$ = 33.6 Hz. UV–Vis (CH_2Cl_2, 10^{-5} M): λ/nm (ε/M^{-1} cm^{-1}) 234 (6.99 × 10^4), 290 (2.91 × 10^4), 300 (2.88 × 10^4), 408 (4.06 × 10^3). ESI (m/z^+): 830 $[C_{46}H_{40}N_3O_2P_2Ru]^+$.

4.9. Anti-M. tuberculosis activity assay

The anti-MTB activity of the compounds was determined by the *Resazurin Microtiter Assay* (REMA) [47]. Stock solutions of the test compounds were prepared in dimethyl sulfoxide (DMSO) and diluted in Middlebrook 7H9 broth (Difco), supplemented with oleic acid, albumin, dextrose and catalase (OADC enrichment - BBL/Becton Dickinson, Sparks, MD, USA), to obtain final drug concentration ranges from 0.15 to 250 μg/mL. The serial dilutions were realized in a Precision XS Microplate Sample Processor (Biotek™). The isoniazid was dissolved in distilled water, as recommended by the manufacturer (Difco laboratories, Detroit, MI, USA), and used as a standard drug. MTB H_{37}Rv ATCC 27294 was grown for 7–10 days in Middlebrook 7H9 broth supplemented with OADC, plus 0.05% Tween 80 to avoid clumps. Cultures were centrifuged for 15 min at 3150× *g*, washed twice, and resuspended in phosphate-buffered saline and aliquots were frozen at −80 °C. After 2 days, an aliquot was thawed to determine the viability and the Colony-Forming Unit (CFU) after freezing. MTB H_{37}Rv (ATCC 27294) was thawed and added to the test compounds, yielding a final testing volume of 200 μL with 2 × 10^4 CFU/mL. Microplates with serial dilutions of each compound were incubated for 7 days at 37 °C, after resazurin was added to test viability. Wells that turned from blue to pink, with the development of fluorescence, indicated growth of bacterial cells, while maintenance of the blue colour indicated bacterial inhibition [25,47]. The fluorescence was read (530 nm excitation filter and 590 nm emission filter) in a SPECTRAfluor Plus (Tecan®) microfluorimeter. The MIC was defined as the lowest concentration resulting in 90% inhibition of growth of MTB [25]. As a standard test, the MIC of isoniazid was determined on each microplate. The acceptable range of isoniazid MIC is from 0.015 to 0.06 μg/mL [25,47]. Each test was set up in triplicate.

4.10. Cytotoxicity assay

In vitro cytotoxicity assays (IC_{50}) were performed on the J774A.1 (ATCC TIB-67) mouse cell line, as recommended by Pavan et al. [3] The cells were routinely maintained in complete medium (RPMI-1640 supplemented with 10% heat-inactivated fetal bovine serum (FBS) plus 100 U/mL penicillin and 100 μg/mL streptomycin), at 37 °C, in a humidified 5% CO_2 atmosphere. After reaching confluence, the cells were detached and counted. For the cytotoxicity assay, 1×10^5 cells/mL were seeded in 200 μL of complete medium in 96-well plates (NUNC™). The plates were incubated at 37 °C under a 5% CO_2 atmosphere for 24 h, to allow cell adhesion prior to drug testing. The compounds were dissolved in DMSO (5%) and subjected to two-fold serial dilution from 1250 to 3.9 μg/mL. Cells were exposed to the compounds at various concentrations for 24 h. Resazurin solution was then added to the cell cultures and incubated for 6 h. Cell respiration, as an indicator of cell viability, was detected by reduction of resazurin to resorufin, whose pink colour and fluorescence indicates cell viability. A persistent blue colour of resazurin is a sign of cell death [25,47]. The fluorescence measurements (530 nm excitation filter and 590 nm emission filter) were performed in a SPECTRAfluor Plus (Tecan) microfluorimeter. The IC_{50} value was defined as the highest drug concentration at which 50% of the cells are viable relative to the control [3]. Each test was set up in triplicate.

4.11. Selectivity index

The selectivity index (SI) was calculated by dividing IC_{50} for the mouse cells by the MIC for the pathogen; if the SI is $\geq$10, the compound is then investigated further [29].

4.12. In vitro infection model

The intracellular anti-MTB activity of the compounds was determined by *in vitro* infection model, as suggested by Snewin et al. [48] MTB Erdmann (ATCC 35801) containing the Luciferase Plasmid (pSMT1) [49] was cultured in Middlebrook 7H9 broth supplemented with OADC and hygromycin (50 μg/mL). The suspension was then seeded on Middlebrook 7H10 (solid medium), supplemented with OADC, for CFU/mL counts. The luminescence (*RLU - Relative Luminescence Units*) of the suspension was read in a SPECTRAfluor Plus (TECAN), after adding the substrates, namely, 0.1 ml of 1% n-decyl aldehyde (Sigma) in ethanol [50], and compared with the CFU/mL. The comparison between RLU/mL and CFU/mL was carried out three times (at 0, 3 and 7 days) (Fig. 4). The J774A.1 (ATCC TIB-67) murine macrophage-like cell line was routinely maintained in RPMI-1640 complete medium (see cytotoxicity assay), at 37 °C and 5% CO_2. After reaching confluence, the cells were detached and counted. For the intracellular anti-MTB activity, 5 x 10^5 cells/mL were seeded in a 24-well plate (NUNC™) (1 mL per well) at 37 °C and 5% CO_2, for 24 h. The plates were incubated at 37 °C under a 5% CO_2 atmosphere for 24 h to allow cell adhesion prior to drug testing. Bacterial suspensions were washed three times in phosphate-buffered saline (PBS) by centrifuging at 2200× *g* for 10 min and resuspended in RPMI-1640 complete medium. Cells were infected by incubation with 1–5 bacteria per cell for 1 h at 37 °C and then washed three times with Hanks balanced salt solution (GIBCO BRL). The total number of cell-associated mycobacteria was initially determined, as follows. J774A.1 cells were lysed by the addition of 1 mL of sterile distilled water containing 0.1% Triton X-100 per well. The bacteria that were internalized in macrophages showed luminescence, confirming the infection. The complexes were diluted in RPMI-1640 complete medium at the following concentrations: MIC value, 4 times higher and 4 times lower than MIC (1 mL per well at each concentration). Our previous studies showed that incubation for 3 days is an optimal period. Thus, the plates were incubated for 3 days at 37 °C and 5% CO_2 and then washed and lysed. The RLU was determined and the percent inhibition by each compound at each concentration was calculated, based on the positive control test. As a standard test, the intracellular inhibition by rifampin was determined (Table 4). Each test was set up in triplicate.

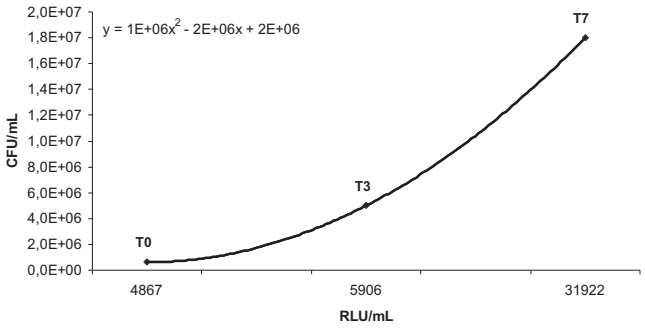

Fig. 4. Growth of MTB Erdmann (ATCC 35801) in 7 days and the comparison between CFU/mL and RLU/mL.

Acknowledgements

This study was supported by CNPq and Fundação de Amparo à Pesquisa do Estado de São Paulo (FAPESP) ref. Process: 2008/10390-2 and 2009/06499-1 and CYTED network RIIDFCM. We thank careful proofreading of the text by Timothy John C. Roberts (M.Sc).

Appendix. Supplementary Material

Crystallographic data for the structural analysis for the complex [Ru(pic)(dppb)(bipy)]$PF_6 \cdot 2H_2O$ (**SCAR 01**) discussed here have been deposited at the Cambridge Crystallographic Data Centre, 12 Union Road, Cambridge, CB2 1EZ, UK and is available on request quoting the deposition number CCDC 817301. These supplementary data can be obtained free of charge via http://www.ccdc.cam.ac.uk/conts/retrieving.html.

References

[1] Scientific Blueprint for TB Drug Development, Global Alliance for TB Drug Development (2009) pp. 26–28.
[2] L.V. Sacks, R.E. Behrman, Developing new drugs for the treatment of drug-resistant tuberculosis: a regulatory perspective, Tuberculosis 88 (2008) 93–100.
[3] F.R. Pavan, P.I.S. Maia, S.R.A. Leite, V.M. Deflon, A.A. Batista, D.N. Sato, S.G. Franzblau, C.Q.F. Leite, Thiosemicarbazones, semicarbazones, dithiocarbazates and hydrazide/hydrazones: anti-*Mycobacterium tuberculosis* activity and cytotoxicity, Eur. J. Med. Chem. 45 (2010) 1898–1905.
[4] MÉDICINS SANS FRONTIÈRES, http://www.msf.or.jp/info/pressreport/pdf/TBpipeline_E.pdf (acessed 08/05/2010).
[5] Z. Ma, C. Lienhardt, H. Mclleron, A.J. Nunn, X. Wang, Global tuberculosis drug development pipeline: the need and the reality, Lancet 5 (2010) 1–10.
[6] D. Sriram, P. Yogeeswari, R. Thirumurugan, Antituberculous activity of some aryl semicarbazone derivatives, Bioorg. Med. Chem. Lett. 4 (2004) 3923–3924.
[7] M.B. Tarallo, C. Urquiola, A. Monge, B.P. Costa, R.R. Ribeiro, A.J. Costa-filho, R.C. Mercader, F.R. Pavan, C.Q.F. Leite, M.H. Torre, D. Gambino, Design of novel iron compounds as potential therapeutic agents against tuberculosis, J. Inorg. Biochem. 104 (2010) 1164–1170.
[8] I. Ott, R. Gust, Non-platinum metal complexes as anti-cancer drugs, Arch. Pharm. Chem. Life Sci. 340 (2007) 117–126.
[9] F.R. Pavan, G.V. Poelhsitz, F.B. do Nascimento, S.R.A. Leite, A.A. Batista, V.M. Deflon, D.N. Sato, S.G. Franzblau, C.Q.F. Leite, Ruthenium (II) phosphine/picolinate complexes as antimycobacterial agents, Eur. J. Med. Chem. 45 (2010) 598–601.
[10] P.I.S. Maia, A. Graminha, F.R. Pavan, C.Q.F. Leite, A.A. Batista, D.F. Back, E.S. Lang, J. Ellena, S.S. Lemos, H.S.S. de Araújo, V.M. Deflon, Palladium(II)

complexes with thiosemicarbazones. Syntheses, characterization, cytotoxicity against breast cancer cells and anti-*Mycobacterium tuberculosis* activity, J. Braz. Chem. Soc. 21 (2010) 1177–1186.
[11] P.I.S. Maia, F.R. Pavan, C.Q.F. Leite, S.S. Lemos, G.F. de Souza, A.A. Batista, O.R. Nascimento, J. Ellena, E.E. Castellano, E. Niquef, V.M. Deflon, Vanadium complexes with thiosemicarbazones: synthesis, characterization, crystal structures and anti-*Mycobacterium tuberculosis* activity, Polyhedron 28 (2009) 398–406.
[12] A.C. Moro, A.E. Mauro, A.V.G. Netto, S.R. Ananias, M.B. Quilles, I.Z. Carlos, F.R. Pavan, C.Q.F. Leite, M. Hörner, Antitumor and antimycobacterial activities of cyclopalladated complexes: X-ray structure of [Pd(C2, N-dmba)(Br)(tu)] (dmba = N, N-dimethylbenzylamine, tu = thiourea), Eur. J. Med. Chem. 44 (2009) 4611–4615.
[13] M.B. Tarallo, A.J. Costa-Filho, E.D. Vieira, A. Monge, C.Q.F. Leite, F.R. Pavan, G. Borthagaray, D. Gambino, M.H. Torre, Research of new mixed-chelate copper complexes with quinoxaline N1, N4-dioxide derivatives and Alanine as ligands, potential antimycobacterial agents, J. Argentine Chem. Soc. 97 (2009) 80–89.
[14] F.B. do Nascimento, G.V. Poelhsitz, F.R. Pavan, D.N. Sato, C.Q.F. Leite, H.S.S. de Araújo, J. Ellena, E.E. Castellano, V.M. Deflon, A.A. Batista, Synthesis, characterization, X-ray structure and *in vitro* antimycobacterial and antitumoral activities of Ru(II) phosphine/diimine complexes containing the SpymMe2 ligand, SpymMe2=4,6-dimethyl-2-mercaptopyrimidine, J. Inorg. Biochem. 102 (2008) 1783–1789.
[15] S.L. Queiroz, A.A. Batista, G. Oliva, M. Gambardella, R.H.A. Santos, K.S. Macfarlane, S.J. Rettig, B.R. James, The reactivity of five-coordinate Ru(II)(1,4-bis(diphenylphosphino)butane) complexes with the N-donor ligands: ammonia, pyridine, 4-substituted pyridines, 2,2-bipyridine, bis(o-pyridil)amine, 1, 10-phenanthroline ,7-diphenyl-1,10-phenanthroline and ethylenediamine, Inorg. Chim. Acta 267 (1998) 209–221.
[16] K.S. MacFarlane, A.M. Joshi, S.J. Rettig, B.R. James, Characterization of five-coordinate ruthenium(II) phosphine complexes by X-ray diffraction and solid-state (31)PCP/MAS NMR studies and their reactivity with sulfoxides and thioethers, Inorg. Chem. 35 (1996) 7304–7310.
[17] P.G. Jessop, S.J. Rettig, C. Lee, B.R. James, (Hydrido)thiolato- and thiolato-carbonylphosphine complexes of ruthenium(II), Inorg. Chem. 30 (1991) 4617–4627.
[18] M.P. de Araujo, E.M.A. Valle, J. Ellena, E.E. Castellano, E.N. dos Santos, A.A. Batista, mer-[$RuCl_3$(P–P)H_2O] (P–P = dppb or diop) as a starting material for the synthesis of binuclear complexes. Crystallographic structures of [(dppb)ClRu–μ(Cl)$_3$–RuCl(dppb)] and [(η^6-C_6H_6)Ru–μ(Cl)$_3$–RuCl(dppb)].: imine hydrogenation using mono- and binuclear ruthenium complexes, Polyhedron 23 (2004) 3163–3172.
[19] G.V. Poelhsitz, R.C. Lima, R.M. Carlos, A.G. Ferreira, A.A. Batista, A.S. de Araujo, J. Ellena, E.E. Castellano, Influence of ligands on the fac (hv)reversible arrow mer isomerization in [RuCl3(NO)(P-P)] complexes, [P-P (Delta)= R2P(CH2)(n) PR2 (n=1-3) and R2P(CH2)POR2, PR2-CH=CH-PR2, R=Ph and (C6H11)(2)P-(CH2)(2)-P(C6H11)(2)], Inorg. Chim. Acta 359 (2006) 2896–2909.
[20] P. Sengupta, R. Dinda, S. Ghosh, W.S. Sheldrick, Synthesis and characterisation of some ruthenium(II) complexes of -N heterocyclic carboxylic acids-X-ray structures of cis-[Ru(PPh3)2(L1)2].2CH3OH and cis-[Ru(PPh3)2(L3H)2] (L1H=pyridine 2-carboxylic acid and L3H2=imidazole 4,5-dicarboxylic acid), Polyhedron 20 (2001) 3349–3354.
[21] K.N. Mitra, S. Choudhury, S. Goswami, S. Peng, A family of mixed ligand complexes of Ru^{II}-L [L = N-aryl-pyridine-2-aldimine], their reactions, isolation and characterization. X-ray crystal structure of [Ru(pic)(L^1)$_2$][ClO_4]· CH_2Cl_2 [pic= 2-picolinate ion], Polyhedron 16 (1997) 1605–1614.
[22] M.O. Santiago, C.L. Donicci Filho, I.S. Moreira, R.M. Carlos, S.L. Queiroz, A.A. Batista, Photochemical isomerization of trans- to cis-[RuCl2(dppb)(4,4-X2-2,2-bipy] (X = -H, -NO2, -Me, -COOH, -SMe, -O=SMe, -Cl, -OMe) complexes, Polyhedron 22 (2003) 3205–3211.
[23] D. Sukanya, R. Prabhakaran, K. Natarajan, Ruthenium(III) complexes of dipicolinic acid with PPh_3/$AsPh_3$ as co-ligand: synthesis and structural characterization, Polyhedron 25 (2006) 2223–2228.
[24] R.F. Winter, B.M. Brunner, T. Scheiring, High-yield syntheses and electrochemistry of cis-[RuCl2(depe)2] and cis-[RuCl(CH3CN)(depe)2]+PF6-, Inorg. Chim. Acta 310 (2000) 21–26.
[25] L.A. Collins, S.G. Franzblau, Microplate alamar blue assay versus BACTEC 460 system for high-Throughput screening of compounds against *Mycobacterium tuberculosis* and *Mycobacterium avium*, Antimicrob. Agents Chemother. 41 (1997) 1004–1009.
[26] R.P. Tripathi, N. Tewari, V.K. Dwivedi, Fighting tuberculosis: an old disease with new challenges, Med. Res. Rev. 25 (2005) 93–131.
[27] M. Protopopova, C. Hanrahan, B. Nikonenko, R. Samala, P. Chen, J. Gearhart, L. Einck, C.A. Nacy, Identification of a new antitubercular drug candidate, SQ109, from a combinatorial library of 1,2-ethylenediamines, J. Antimicrob. Chemother. 56 (2005) 968–974.
[28] K. Andries, P. Verhasselt, J. Guillemont, H.W.H. Gohlmann, J.M. Neefs, H. Winkler, J.V. Gestel, P. Timmerman, M. Zhu, E. Lee, P. Williams, D. de Chaffoy, E. Huitric, S. Hoffner, E. Cambau, C. Truffot-Pernot, N. Lounis, V.A. Jarlier, Diarylquinoline drug active on the ATP Synthase of *Mycobacterium tuberculosis*, Science 307 (2005) 223–227.
[29] I. Orme, J. Secrist, S. Anathan, C. Kwong, J. Maddry, R. Reynolds, A. Poffenberger, M. Michael, L. Miller, J. Krahenbuh, L. Adams, A. Biswas, S. Franzblau, D. Rouse, D. Winfield, J. Brooks, Search for new drugs for treatment of tuberculosis, Antimicrob. Agents Chemother. 45 (2001) 1943–1946.
[30] O. Novakova, H. Chen, O. Vrana, A. Rodger, P.J. Sadler, V. Brabec, DNA interactions of monofunctional organometallic ruthenium(ii) antitumor complexes in cell-free media, Biochemistry 42 (2003) 11544–11554.
[31] C. Gossens, I. Tavernelli, U. Rothlisberger, DNA structural distortions induced by ruthenium-arene anticancer compounds, J. Am. Chem. Soc. 130 (2008) 10921–10928.
[32] S. Das, S. Sinha, R. Britto, K. Somasundaram, A.G. Samuelson, Cytotoxicity of half sandwich ruthenium(II) complexes with strong hydrogen bond acceptor ligands and their mechanism of action cytotoxicity of half sandwich ruthenium(II) complexes with strong hydrogen bond acceptor ligands and their mechanism of action, J. Inorg. Biochem. 104 (2010) 93–104.
[33] Based on ZINDO/1 calculation performed by one of us. Not published results.
[34] C.G. Hartinger, S. Zorbas-Seifried, M.A. Jakupec, B. Kynast, H. Zorbas, B.K. Keppler, From bench to bedside-preclinical and early clinical development of the anticancer agent indazolium trans-[tetrachlorobis(1H-indazole) ruthenate(III)] (KP1019 or FFC14A, J. Inorg. Biochem. 100 (2006) 891–904.
[35] I. Bratsos, D. Urankar, E. Zangrando, P. Genova-Kalou, J. Kosmrli, E. Alessio, I. Turel, 1-(2-Picolyl)-substituted 1,2,3-triazole as novel chelating ligand for the preparation of ruthenium complexes with potential anticancer activity, Dalton Trans. 40 (2011) 5188–5189.
[36] M. Groessl, O. Zava, P.J. Dyson, Cellular uptake and subcellular distribution of ruthenium-based metallodrugs under clinical investigation versus cisplatin, Metallomics 3 (2011) 591–599.
[37] M.C.R. Monteiro, F.B. Nascimento, E.M.A. Valle, J. Ellena, E.E. Castellano, A.A. Batista, S.P. Machado, Experimental and theoretical study of the kinetics of dissociation in cis-[RuCl2(P-P)(N-N)] type complexes, J. Braz. Chem. Soc. 21 (2010) 1992–1999.
[38] E.M.A. Valle, B.A.V. Lima, A.G. Ferreira, F.B. Nascimento, V.M. Deflon, I.C.N. Diógenes, U. Abram, J. Ellena, E.E. Castellano, A.A. Batista, Driving forces in substitution reactions of octahedral complexes: the influence of the competitive effect, Polyhedron 28 (2009) 3473–3478.
[39] A. Garcia-Raso, J.J. Fiol, A. Tasada, M.J. Prieto, V. Moreno, I. Mata, E. Molins, T. Bunic, A. Golobic, I. Turel, Ruthenium complexes with purine derivatives: syntheses, structural characterization and preliminary studies with plasmidic DNA, Inorg. Chem. Commun. 8 (2005) 800–804.
[40] L. Otero, M. Vieites, L. Boiani, A. Denicola, C. Rigol, L. Opazo, C. Olea-Azar, J.D. Maya, A. Morello, R.L. Krauth-Siegel, O.E. Piro, E. Castellano, M. González, D. Gambino, H. Cerecetto, Novel antitrypanosomal agents based on palladium nitrofurylthiosemicarbazone complexes: DNA and redo metabolism as potential therapeutical targets, J. Med. Chem. 49 (2006) 3322–3331.
[41] R.E. Mahnken, M.A. Billadeau, E.P. Nikonowicz, H. Morrison, Development of photo cis-platinum reagents, reaction of cis-dichlorobis(1,10-phenanthroline) rhodium(III) with calf thymus DNA, nucleotides and nucleosides, J. Am. Chem. Soc. 114 (1992) 9253–9265.
[42] Enraf-Nonius, Collect, Nonius BV, Delft, The Netherlands, 1997–2000.
[43] Z. Otwinowski, W. Minor, Processing of X-ray diffraction data collected in Oscillation mode. in: C.W. CarterJr., R.M. Sweet (Eds.), Methods in Enzymology. Academic Press., New York, 1997, pp. 307–326.
[44] R.H. Blessing, An empirical correction for absorption anisotropy, Acta. Crystallogr. Sect. A 51 (1995) 33–38.
[45] G.M. Sheldrick, SHELXS-97. Program for Crystal Structure Resolution. University of Göttingen, Göttingen, Germany, 1997.
[46] G.M. Sheldrick, SHELXL-97. Program for Crystal Structures Analysis. University of Göttingen, Göttingen, Germany, 1997.
[47] J.C. Palomino, A. Martin, M. Camacho, H. Guerra, J. Swings, F. Portaels, Resazurin microtiter assay plate: simple and inexpensive method for detection of drug resistance in *Mycobacterium tuberculosis*, Antimicrob. Agents Chemoter 46 (2002) 2720–2722.
[48] V.A. Snewin, M.P. Gares, P.O. Gaora, Z. Hasan, I.N. Brown, D.B. Young, Assessment of immunity to mycobacterial infection with luciferase reporter constructs, Infect. Immun. 67 (1999) 4586–4593.
[49] G. Rook, B. Bloom, Mechanisms of pathogenesis in tuberculosis. in: B. Bloom (Ed.), Tuberculosis: pathogenesis, protection and control. ASM Press., Washington D.C, 1994, pp. 485–501.
[50] T.M. Arain, A.E. Resconi, D.C. Singh, K. Stover, Reporter gene technology to assess activity of antimycobacterial agents in macrophages, Antimicrob. Agents Chemother. 40 (1996) 1542–1544.